Scheme I

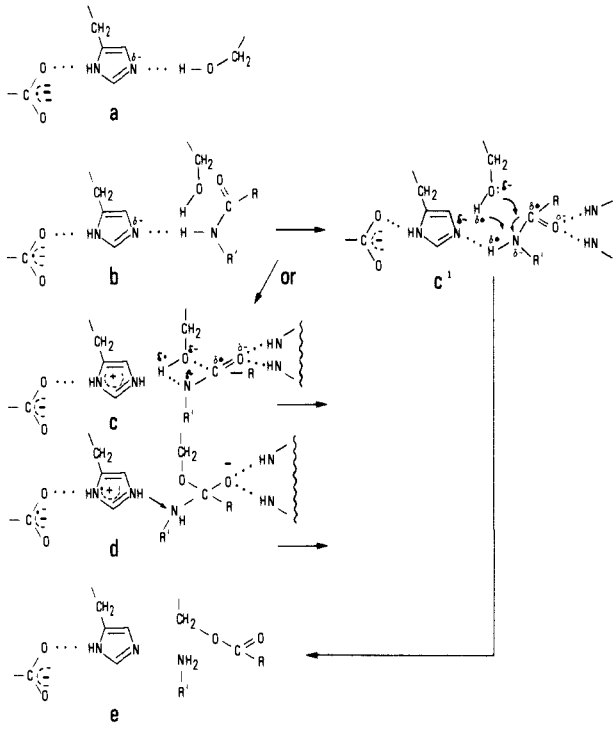

The actual mechanism may involve therefore a complex sequence of proton transfers at this stage.

In summary, the essential features of the suggested mechanism are the negative charge in the aspartate–imidazole complex and the strong intrinsic acidity of the substrate peptide NH. Together, these features lead to a mechanism equivalent to the base-catalyzed hydrolysis of the peptide. This is reasonable since, in essence, COO^- is a strong base and the substrate peptide link is a strong intrinsic acid.

In discussing these details, it is recognized that the lowest energy path may not be available in the enzyme because of steric constraints, and multiple interaction effects may also alter relative energies. In this case, the present lowest energy mechanism may not apply in natural enzymes but may be of interest in synthetic enzymes where lowest energy paths may be realized.

Conclusion

Data from ion clusters directly involving model biomolecules are applied to obtain quantitative estimates of ionic interactions in protein environments. The clustering studies show that protein environments can solvate ionic species substantially. Two amide links of a peptide backbone can stabilize an anion by 45 kcal/mol, and a cation by a similar amount, so that four such peptide units can stabilize a cation–anion pair at infinite separation by 90–110 kcal/mol. Together with further stabilization by nearby ionic and polar groups and water molecules, the protein can therefore provide a strongly stabilizing environment for ionic intermediates.

In the special case of serine proteases, the ionic intermediate involves a carboxylate stabilized by four hydrogen bonds, which may contribute as much as 60 kcal/mol, and a tetrahedral oxyanion intermediate bonded to two peptide backbone NH groups, which can contribute over 30 kcal/mol. These latter interactions are therefore substantial and may indeed be the main catalytic factor as suggested by Warshel and Russell. Further, the present results and considerations of intrinsic acidities suggest an alternative proteolytic mechanism where a substrate amide proton is transferred to the imidazole center of the enzyme.

The present data display the usual correlation between hydrogen bond strength and acidities. The hydrogen donor strength of peptide link in ionic hydrogen bonds is therefore enhanced by its high intrinsic acidity. The ion–neutral bond between aspartate and imidazole in enzyme centers is also enhanced by the high intrinsic acidity of imidazole. Further, we found similarly high intrinsic acidity in another essential hydrogen donor, i.e., aminopyrimidine that models nucleic base components. In addition to its effect in ionic systems, increased intrinsic acidities also strengthen key neutral hydrogen bonds. The intrinsic acidity therefore emerges as a unifying property that may have affected the natural selection of donor molecules for essential biological hydrogen bonds in both ionic and neutral systems.

Acknowledgment. I thank Dr. M. Krauss and Dr. A. Warshel for helpful comments and a critical review of this work.

Time-Resolved Slow Dissociation of Benzonitrile Ions by Trapped-Ion Ion Cyclotron Resonance Photodissociation

Hun Young So and Robert C. Dunbar*

Contribution from the Chemistry Department, Case Western Reserve University, Cleveland, Ohio 44106. *Received September 16, 1987*

Abstract: Benzonitrile ions were photodissociated, showing loss of HCN, by single pulses of 308-nm light in the ion cyclotron resonance ion trap. The extent of dissociation following the laser pulse was time resolved, giving a typical time constant of 200 μs for dissociation. The time-resolved photodissociation curve was found to follow very well the behavior expected from extrapolation (via RRKM calculations) of previous dissociation rate measurements in the 1–10-μs regime. It was concluded that a statistical, RRKM theoretical description applies to this dissociation process down at least to rates as slow as 10^3 s^{-1}.

Ion-trap methods have made possible the study of chemical processes in isolated molecules on unprecedentedly long time scales. The study of infrared–fluorescent relaxation on a time scale of tens or hundreds of milliseconds is an outstanding achievement of this approach.[1] Recently the time-resolved observation of the dissociation of chlorobenzene ions on a time scale of tens of microseconds in the ion cyclotron resonance (ICR) ion trap was described.[2] We describe here the a time-resolved study of dissociation of benzonitrile ions by the same technique but on a longer time scale. We believe this to be the slowest unimolecular dissociation process whose time profile has ever been displayed for

(1) (a) Dunbar, R. C.; Chen, J. H.; So, H. Y.; Asamoto, B. *J. chem. Phys.* **1987**, *86*, 2081. (b) Asamoto, B.; Dunbar, R. C. *J. Phys. Chem.* **1987**, *91*, 2804.

(2) Dunbar, R. C. *J. Phys. Chem.* **1987**, *91*, 2801.

0002-7863/88/1510-3080$01.50/0

energetically well defined molecules.

Extensive attention has been given to the phenomenon of relatively slow dissociation in polyatomic molecules, and a satisfactory understanding has developed in terms of a statistically governed energy-pooling mechanism, quantified in quasi-equilibrium theory, RRKM theory,[3] or phase-space theory.[4] Slow dissociation near threshold is the cause of the "kinetic shift" in mass spectrometric appearance potential measurements,[5] and it is by now clearly recognized that in some molecules, of which benzonitrile ion is a good example, near-threshold dissociation is much slower than typical mass spectrometer time scales. The effect of such slow dissociations on appearance energies has been explored with ion-trapping techniques on time scales as long as milliseconds,[6-8] and the presence and importance of these large kinetic shifts have been amply shown and characterized, although the actual dissociation processes have not been displayed as a function of time.

The lowest energy fragmentation of benzonitrile is the reaction

$$C_6H_5CN^+ \rightarrow C_6H_4^+ + HNC \qquad (1)$$

which obviously involves a substantial rearrangement. There have been three principle studies of the kinetics of this fragmentation, with control over the ion internal energy, on a time scale of a few microseconds. The charge-exchange ionization study of Andlauer and Ottinger[9] gave the correct shape for the rate–energy curve but was found later to have a 0.4-eV error in the absolute energy scale, due to excess energy deposition by the high-speed charge-transfer reagent ions. Eland and Schulte[10] used photoionization with coincidence determination of the ejected electron energy and deconvoluted the time-of-flight distribution of the product ions to extract an average dissociation rate for parent ions during the time spent in the acceleration region. This technique yielded reliable values of average rate constant versus internal energy (averaged over the thermal energy distribution) at four rate values between 3×10^5 and 3×10^6 s^{-1}. The later experiment of Rosenstock, Stockbauer, and Parr[11] also used photoionization with coincidence electron energy selection, but instead of measuring the dissociation during the flight time, they sampled the extent of ion fragmentation after a known residence time in the source. This was done with three residence times between 1 and 6 μs, over a range of photon energies in each case, yielding a large amount of reliable rate-energy information for ions in the $(2-10) \times 10^5$ s^{-1} fragmentation rate regime. As is the preference of this group, Rosentock et al. treated their results by a detailed fitting procedure to RRKM calculated curves, presenting an overall fitted rate–energy curve rather than individual experimental rate–energy points. Their curve is in excellent agreement with Eland and Schulte's points.

Gordon and Reid, using an ion trapping technique, studied the dissociation on a millisecond time scale.[6] The results were displayed in terms of appearance energies for $C_6H_4^+$ as a function of trapping time and clearly showed that dissociations on a time scale of hundreds of microseconds were significant. However, the energy-disperse nature of the electron-impact ionization used precluded the quantitative measurement of the rate–energy curve in the slow-dissociation region.

The quantitative understanding of this dissociation in the low-energy region and the assignment of the dissociation threshold energy both rest on the extrapolation, via RRKM theory, of the reliable results around 10^6 s^{-1} into the slow-dissociation region. RRKM theory has had striking success in such applications,[12] but in this case it is open to some uncertainty, because this dissociation involves a major structural rearrangement. The transition state is certainly tight, but its structure can only be speculative. It is thus of particular value to use the ICR photodissociation method to give direct experimental confirmation of the expected dissociation rate at much lower energies and much slower rates.

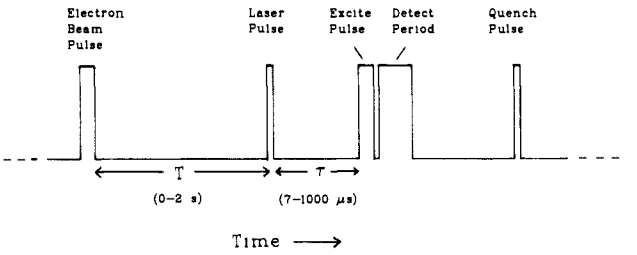

Figure 1. Pulse sequence for time-resolved ICR photodissociation. In this work, the excimer laser pulse was very short (less than 10 ns), the excite pulse was 30–35 μs, and the detect pulse was 1–2 ms.

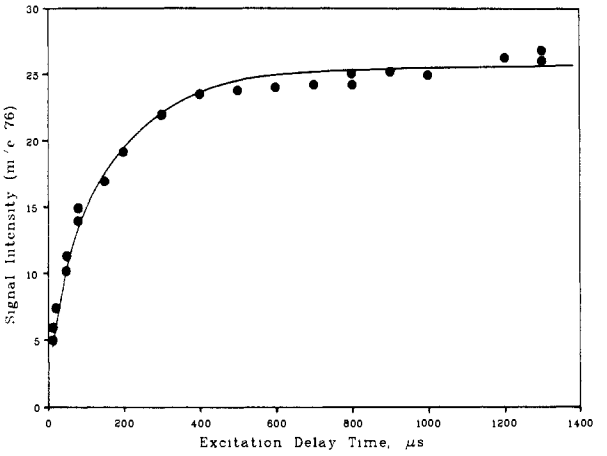

Figure 2. Time-resolved dissociation curve for benzonitrile ions. The plotted points are the signal intensity for $C_6H_4^+$ at m/e 76 as a function of delay time τ after the laser pulse. The solid line is the calculated curve based on the rate–energy curve of Figure 3 and the 350-K thermal distribution of Figure 4.

Experimental Section

The experimental details of the time-resolved ICR photodissociation technique were described in the report on chlorobenzene ion,[2] and the technique used here was essentially the same. As shown in Figure 1, the sequence of events in the ICR cell consists of (1) ion formation by electron impact, (2) a period (typically 2 s) for thermalization of the parent ions, (3) firing of the excimer laser pulse, (4) the delay τ during which dissociation proceeds, (5) firing of the rf excite pulse to give cyclotron excitation to those daughter ions present at the end of the delay τ, (6) acquisition of the ICR transient, which is processed to give the daughter ion abundance, and (7) purging of the cell to initiate a new pulse cycle.

As was discussed previously,[2] the time resolution of this technique is determined by the length of the rf excite pulse, while the ICR mass resolution for daughter ion detection is limited only by the length of the ICR transient (and by inhomogeneous line-broadening effects). In the present work, the time-resolution demands were less stringent than with chlorobenzene ions, and an excite-pulse length of 30 or 35 μs was normally used at about 10 V rf amplitude.

A Lumonics excimer laser was used with XeCl, giving single pulses at 308 nm, which illuminated the ICR cell with a laser spot of the order of 1 cm^2 in area. Photodissociation at 308 nm proceeds with good cross section, and an extent of dissociation at 10% was readily achieved with a 50–100-mJ laser pulse.

Pressure was measured by ionization gauge; on the basis of the study of Georgiadis and Bartmess,[13] the true pressure was taken as 6 times less

(3) Forst, W. *Theory of Unimolecular Reactions*; Academic: New York, 1973. Robinson, P. J.; Holbrook, K. A. *Unimolecular Reactions*; Wiley-Interscience: New York, 1972.
(4) Chesnavich, W. J.; Bowers, M. T. *J. Am. Chem. Soc.* **1977**, *99*, 1705.
(5) Chupka, W. A. *J. Chem. Phys.* **1959**, *30*, 191.
(6) Gordon, S. M.; Reid, N. W. *Int. J. Mass Spectrom. Ion Phys.* **1975**, *18*, 379.
(7) Gefen, S.; Lifshitz, C. *Int. J. Mass Spectrom. Ion Processes* **1984**, *58*, 251. Malinovich, Y.; Arakawa, R.; Haase, G.; Lifshitz, C. *J. Phys. Chem.* **1985**, *89*, 2253.
(8) Gross, M. L. *Org. Mass Spectrom.* **1972**, *6*, 827.
(9) Andlauer, B.; Ottinger, Ch. *J. Chem. Phys.* **1971**, *55*, 1471.
(10) Eland, J. H. D.; Schulte, H. *J. Chem. Phys.* **1975**, *62*, 3835.
(11) Rosenstock, H. M.; Stockbauer, R.; Parr, A. C. *J. Chem. Phys.* **1980**, *77*, 745.
(12) Dannacher, J.; Rosenstock, H. M.; Buff, R.; Parr, A. C.; Stockbauer, R.; Bombach, R.; Stadelmann, J.-P. *Chem. Phys.* **1983**, *75*, 23.
(13) Bartmess, J. E.; Georgiadis, R. M. *Vacuum* **1983**, *33*, 149.

than the ionization gauge reading for benzonitrile. The nominal electron energy was 12–13 eV. The trapping voltage was 3–4 V; this gives a trap depth of more than 1 eV,[14] and it was considered very unlikely that any fragment ions in this experiment would have sufficient kinetic energy to escape the trap.

Results and Discussion

Figure 2 displays a set of time-resolved dissociation results for benzonitrile ion. The delay time between ion formation and the laser pulse was 2 s at 2.5×10^{-8} T, which, as will become clear from the following discussion, is sufficient time for complete ion thermalization.

We will discuss these results from two points of view. First, these are among the first direct experimental observations of a polyatomic dissociation profile on a millisecond time scale, and it is interesting to consider the implications for slow dissociations. Second, the existing thermochemical picture of this dissociation comes from fitting RRKM calculations to dissociation rate measurements in the few-microsecond regime, and both the validity of the RRKM rate calculations and the accuracy of the thermochemistry can be given much greater confidence through testing against the present rate results.

Time-Resolved Curve. It is seen from Figure 2 that the characteristic dissociation time for these ions is about 200 μs ($k = 5 \times 10^3$ s^{-1}). The internal energy of the ions is the 4.03 eV of the laser photons plus the thermal energy at 350 K; the most probable internal energy is 4.10 eV. The accepted value for the dissociation threshold is 3.02 eV,[11] so the ions typically are 1.08 eV above threshold. To be more precise, the ions have a distribution of energies and relaxation rates corresponding to a thermal population at about 350 K; most (about two-thirds) of the ions have internal energies between 4.03 and 4.18 eV, corresponding to dissociation rates between 5×10^3 and 1×10^4 s^{-1}. This is an exceptionally slow dissociation for such a large excess internal energy above threshold; contributing to making it slow are the extensive molecular rearrangement required during dissociation and the high activation energy (giving a large density of states for the energized molecule). This would be a favorable ion for observation of very slow dissociation much nearer threshold.[15] (About 100 s^{-1} would be expected to be the slowest rate that could compete with IR radiative relaxation.) However, the present experimental technique will be difficult near threshold because of the low optical absorption cross section in the range 3–4 eV (300–400 nm).[16]

Dissociation Rates and Thermochemistry. Rosenstock et al.[11] have calculated the rate–energy function for this dissociation process and have used dissociative photoionization yields at various delay times in the 1–6-μs region to calibrate and check the calculations in the $k = 5 \times 10^5$ s^{-1} region. The calculations were further checked and confirmed by excellent agreement with Eland and Schulte's coincidence measurements[10] over the range (3–30) $\times 10^5$ s^{-1}. The most straightforward approach to assessing the quantitative significance of our results, which pertain to a rate regime 2 orders of magnitude slower than these previous studies, is to extrapolate the calculated rate–energy curve of Rosenstock et al. into the relevant rate–energy region and see whether our results are compatible with these extrapolated rates.

In order to carry the rate–energy curve of Rosenstock et al. into the 10^3 s^{-1} range, an RRKM calculation was carried out,[3] with the parameters described by Rosenstock et al.[11] (the case without external rotations with $E_{act} = 3.015$ eV), by using the steepest descents method to evaluate the state densities.[17] Excellent agreement was found with their curve in the region of overlap, and the extended rate–energy curve from this calculation is shown in Figure 3.

The thermal distribution of internal vibrational energies was calculated at 350 K (and also at 375 K for use in Figure 5 below), by using state densities from the RRKM calculation, as shown

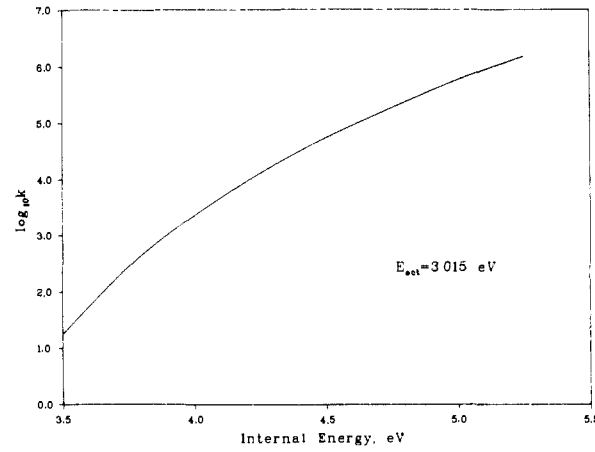

Figure 3. Rate–energy curve for benzonitrile ion dissociation from the RRKM calculation.

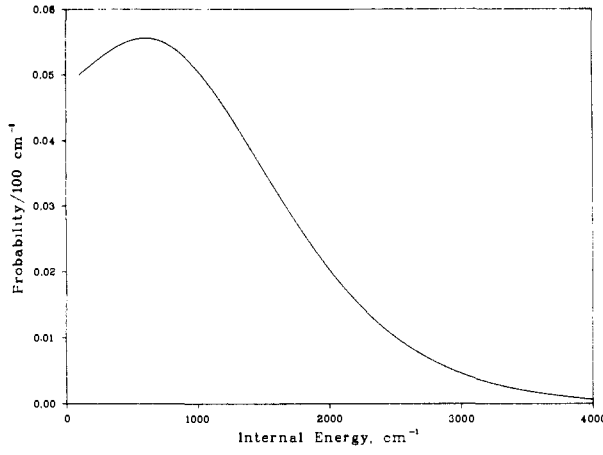

Figure 4. Thermal distribution of vibrational internal energy for benzonitrile at 350 K, using the vibrational frequencies cited in ref 4.

in Figure 4. The time-resolved photodissociation for 4.03-eV photon excitation was then calculated by convoluting the thermal distribution of photoexcited ion energies with the time-resolved ICR signal equation:[2]

$$I(B^+) = C\{\Delta + (1/k)\exp(-k\tau)[\exp(-k\Delta) - 1]\} \quad (2)$$

where $I(B^+)$ is the ICR signal for the product ion B^+ with the excite pulse at a delay time τ after the laser pulse, Δ is the length of the rf excite pulse, k is the unimolecular dissociation rate constant, and C is a constant. For given temperature and given rate–energy function, the constant C is the only adjustable parameter and is fixed to give the observed signal level at long delay times. The predicted 350 K dissociation curve is drawn in Figure 2.

It is seen that the predicted and observed dissociation curves are in excellent agreement. This is a strong result: It indicates that the rate–energy curve of Figure 3 is correct both in the region around 10^6 s^{-1} tested by previous experiments and also in the region around 3×10^3 tested by the present experiment. This in turn strongly indicates the validity of the RRKM dissociation picture for this ion for rates as slow as 10^3 s^{-1} and gives strong inferential support to the 3.02 eV activation energy assigned by Rosenstock et al. to the process.

Thermalization. The ion-dissociation rate is very sensitive to the internal energy, so it is important to assure thermalization of the ions to a well-known temperature before photoexcitation. Previous work on chlorobenzene ion[2] showed that the effective temperature of our ICR cell with its continuously running hot filament is around 350 K, which is taken as the temperature the ions will have when thermalization is complete. To clarify the extent of thermalization of the target ions, the data of Figure 5 show curves for three delay times between the electron-beam pulse

(14) Dunbar, R. C.; Chen, J. H.; Hays, J. D. *Int. J. Mass Spectrom. Ion Processes* **1984**, *57*, 39.
(15) Dunbar, R. C. *Int. J. Mass Spectrom. Ion Processes* **1983**, *54*, 109.
(16) Orlowski, T. E.; Freiser, B. S.; Beauchamp, J. L. *Chem. Phys.* **1976**, *16*, 439.
(17) Forst, W. *Chem. Rev.* **1971**, *71*, 339.

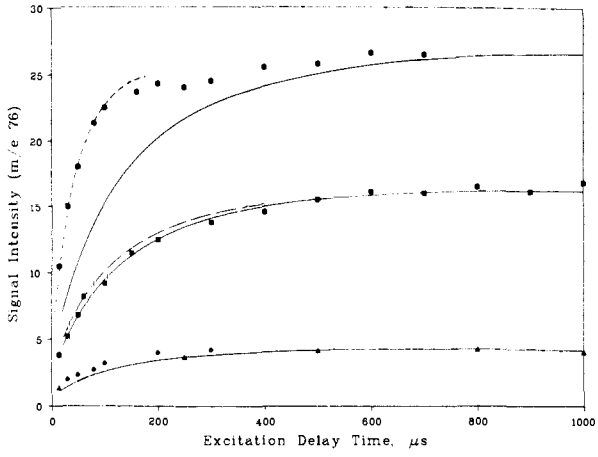

Figure 5. Dissociation curves for three values of the ion-cooling time T: 0.7 s (●), 1.2 s (■), and 2.0 s (▲). The curves drawn are as follows: (—) calculated curves for 350 K parent ions, (- - -) calculated curve assuming a superthermal excess energy of 1400 cm^{-1}, (– –) calculated curve for 375 K parent ions.

and the laser pulse, at fairly low pressure (3×10^{-8} Torr, corresponding to a collision rate of about 1 s^{-1}). The calculated curves (solid lines) are drawn assuming complete thermalization at 350 K. Dissociation appears noticeably faster than expected at 0.7 s, while at 1.2 and 2.0 s the data match the 350 K curves reasonably well. It appears that the ions retain some excess internal energy at 0.7 s after their formation; as an indication of the order of magnitude of excess energy involved, the dashed curve plotted with the 0.7-s data is calculated, assuming that the ions retain 1400 cm^{-1} (0.17 eV) of internal energy in excess of thermal energy, giving a reasonable fit to these data. The agreement with the expected RRKM curves with longer thermalization times gives confidence that the ions observed after 2-s thermalization are not more than a few hundred cm^{-1} at most above 350-K thermal internal energy.

As an indication of how sensitive these results are to the internal energy or temperature of the ion, a calculation was made of the predicted dissociation curve at an ion internal temperature of 375 K. This is shown along with the 350 K curve with the 1.2-s data in Figure 5. It is seen that the change of 25 K in assumed temperature makes a noticeable difference in the curve but that the fit to the data is still not bad. In terms of internal energy, this 25-K increase represents a 200 cm^{-1} rise in most probable internal energy (from 600 cm^{-1} at 350 K to 800 cm^{-1} at 375 K), increasing the dissociation rate by a factor of 1.2. With the level of precision and reproducibility of the present data, this difference of 25 K does not change the fit to the data outside of experimental uncertainty, but a change of 75 K in the assumed ion temperature (or a change in the assumed activation energy by 600 cm^{-1} (0.07 eV)) would clearly not allow a reasonable fit.

Conclusions

We have displayed the time-resolved appearance spectrum of the $C_6H_4^+$ fragment ion from photodissociation of benzonitrile parent ion. Thorough thermalization of the ions before the laser pulse, along with the precisely known energy of the 308-nm photon, give excellent control of the internal energy of the dissociating parent ion. The millisecond time scale of observation is an interesting advance into a domain of slow fragmentation reactions, which have not been accessible with isolated, collision-free molecules. The ICR trapped-ion techniques used here have spanned the range from 10 to 1500 μs in the observation of product formation following the laser pulse, and there is no intrinsic barrier to extending the observations to seconds of dissociation time, if any reactions that slow can be found.

The observed dissociation of benzonitrile ion at around 4.05-eV internal energy shows a typical time constant of 200 μs. While this experiment is in a rate regime 2 orders of magnitude slower than previous quantitative rate studies of this fragmentation, the present results are in complete accord with the predictions of the statistical, RRKM theory, which successfully accounted for observations at higher internal energies. This agreement gives indirect but solid confirmation, within ±0.07 eV, of the previously assigned activation energy for the fragmentation.

Acknowledgment. The support of the National Science Foundation and of the donors of the Petroleum Research Fund, administered by the American Chemical Society, is gratefully acknowledged.